
American Association of Physics Teachers
Explore the AAPT Career Center – access hundreds of physics education and other STEM teaching jobs at two-year and four-year colleges and universities.
http://jobs.aapt.org

Analytical solution of gravity tunnels through an inhomogeneous Earth

Stefan Isermann
45259 Essen, Germany

(Received 14 May 2018; accepted 20 October 2018)

A piecewise linear approximation of the Preliminary reference Earth model (PREM) is used for the Earth's velocity profile. The analytical solution derived for the motion on the shortest path and the path of fastest descent corresponds to the direct numerical integration of the PREM. This explains why traversal times can be approximated by the assumption of constant gravity, while the gravity of the Earth is certainly not constant.
https://doi.org/10.1119/1.5075717

I. INTRODUCTION

Considerations of a hypothetical gravitational tunnel through the Earth have a long history, outlined by Selmke[1] in a short note. The analytical solution of a gravity tunnel for a homogeneous gravitating sphere is well known and is left as an exercise in classical mechanics textbooks.[2] In 1966, Venezian[3] pointed out that the solution of the brachistochrone, the path that takes the least time between two points, is simple enough to be expressed in terms of elementary functions instead of as a numerical result. Taking into account more realistic models of the Earth's density distribution calculations, mainly numerical, are performed to obtain more accurate traversal times. In Ref. 4, numerical calculations are made for a polytrope model of the Earth's interior, a model in which the pressure varies as a power of the density. The proposed model fits better than the assumption of constant density, but the results differ significantly from numerical calculations presented in Ref. 5 based on the more realistic and widely used Preliminary Reference Earth Model (PREM).[6] Numerical results in Ref. 5 are compared with analytical calculations provided that gravity or density is constant. It is found that, assuming constant gravity, traversal times are nearly the same. But that model would require a singularity with infinite density at the center of the earth.

It is shown that an analytical solution of the non-uniform Earth is more complex but still simple enough to be expressed in a closed form (trigonometric functions and Legendre elliptical integrals).

II. VELOCITY PROFILE

We neglect all complicating effects such as drag caused by a non-evacuated tunnel or by guiding rails, as discussed in Ref. 7, or the rotation of the earth, as discussed in Ref. 8; the motion through the tunnel is only considered to be dependent on local gravity. Under these assumptions, knowledge of the path s and the velocity profile $v(r)$ is sufficient to investigate the time-dependent solution of motion in differently shaped gravitational tunnels through the Earth

$$t = \int \frac{ds}{v(r)} . \tag{1}$$

For radial symmetry, the velocity profile of the Earth is completely determined by its density distribution $\rho(\vec{r})$. In spherical coordinates the Poisson equation, the differential form of Gauss's law, reads

$$\frac{1}{r^2}\frac{\partial}{\partial r}\left(r^2 \frac{\partial \phi}{\partial r}\right) = 4\pi G \rho(r), \tag{2}$$

where ϕ is the gravitational potential and G is the gravitational constant. Conservation of energy for a radially moving particle gives

$$\frac{v(r)^2}{2} = 4\pi G \int_r^R \frac{dr'}{r'^2} \int_0^{r'} dr'' r''^2 \rho(r'') . \tag{3}$$

It is assumed that the velocity at the surface $v(r=R)$ is zero. From Eq. (1), we see that the velocity dependence on r results from a double integration of the density profile. Even when the density is discontinuous, the velocity profile is smooth (actually it is of class C^1, i.e., the first derivative exists and is continuous). Furthermore, the position as a function of time, $s(t)$, is of class C^2 provided the velocity is of class C^1. With

$$g(r) = \frac{4\pi G}{r^2} \int_0^r dr' r'^2 \rho(r') = \frac{GM(r)}{r^2}, \tag{4}$$

one may rewrite Eq. (3) as

$$\frac{v(r)^2}{2} = \int_r^R dr' g(r'), \tag{5}$$

where $g(r)$ is the absolute value of the gravitational acceleration $\mathbf{g} = -g(r)\mathbf{e_r}$ pointing towards the center of the Earth with decreasing mass $M(r)$.

Dziewonski and Anderson[6] describe a model (PREM) in which the Earth is divided into regions within which properties such as the density vary smoothly. In the mathematical abstraction of this model, variations are approximated by low-order polynomials (up to order 3) in the normalized radius.

Input parameters constraining the PREM are the radius of the Earth $R = 6371$ km, the mass M and the moment of inertia, leading to a gravitational acceleration at the surface of $g = 9.8156\,\mathrm{ms}^{-2}$. In the following calculations, we use normalized variables, so that distance is measured in units of radius R, time in units of $(R/g)^{1/2}$ and velocity in units of $(gR)^{1/2}$.

With the coefficients of the polynomials in the normalized radius given by the PREM,[6] the integrations in Eqs. (3)–(5) can be carried out analytically. The analytic solution of Eq. (4) is shown in Fig. 1. Gravity slightly increases from the surface to a maximum of $g_{max} \approx 1.09$ at the transition from

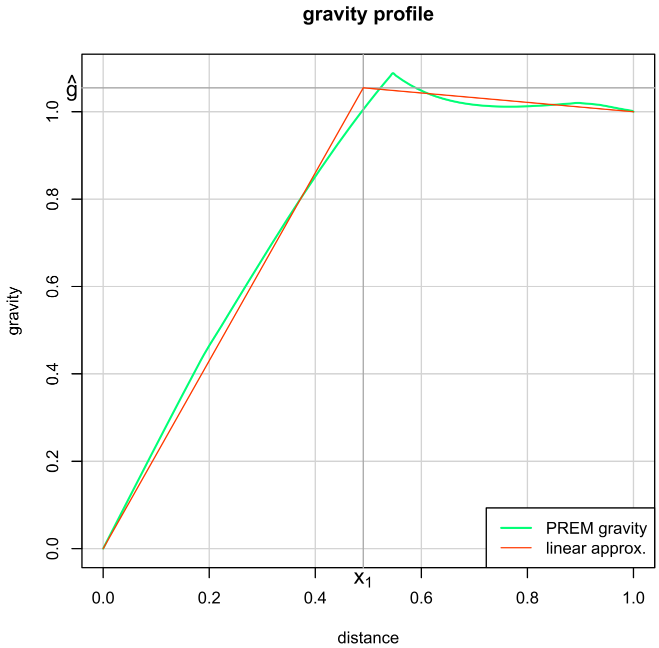

Fig. 1. The gravity profile of the Earth deduced from PREM and a linear approximation with distance from the center and gravitation in normalized units g and R.

the lower mantle to the outer core at $x = 3480/6371 \approx 0.55$. Then it drops rapidly to zero at the center of the Earth.

It seems reasonable to approximate the gravity profile by a piecewise linear model, slightly increasing from the surface up to the outer core and then decreasing to the center of the Earth

$$g_{\text{appr.}}(x) = \begin{cases} 1 + \mu(1-x) & 1 \geq x \geq x_1, \\ \dfrac{\hat{g}}{x_1} x & x_1 \geq x \geq 0, \end{cases}$$

$$\text{where } \mu = \frac{\hat{g} - 1}{x_1 - 1}\,. \tag{6}$$

In this linear approximation, gravity increases linearly with the gradient $\mu > 0$ from its value 1 at the surface to a maximum value $\hat{g}$ at a radius x_1 in the region of the outer core and then drops linearly to zero as indicated in Fig. 1. The parameters of this approximation naturally describe both the case of constant gravity $g_{\text{appr.}}(x, x_1 = 0, \hat{g} = 1) = 1$ with $\mu = 0$ and constant density $g_{\text{appr.}}(x, x_1 = 0, \hat{g} = 0) = x$ with $\mu = -1$. (It should be noted that any pair of parameters with $x_1 = \hat{g}$ represents the case of constant density with $\mu = -1$.)

In further calculations, we are only interested in the radial velocity profile that results directly from the integration of $g_{\text{appr.}}$ according to Eq. (5)

$$v(x, x_1, \hat{g}) = \begin{cases} \sqrt{(1-x)\big(2 + \mu(1-x)\big)} & 1 \geq x \geq x_1, \\ \sqrt{1 + \hat{g} - x_1 - \dfrac{\hat{g}}{x_1} x^2} & x_1 \geq x \geq 0. \end{cases} \tag{7}$$

As above the velocity profiles of constant gravity $v(x, x_1 = 0, \hat{g} = 1) = (2(1-x))^{1/2}$ and constant density $v(x, x_1 = 0, \hat{g} = 0) = (1 - x^2)^{1/2}$ can be identified. Note that the velocity near the surface ($1 - x \ll 1$) does not depend on the gradient μ, i.e., increasing or decreasing gravity, and is equal to the velocity profile for constant gravity $v(x) = (2(1-x))^{1/2}$.

The parameters x_1 and $\hat{g}$ are chosen so that the integrand in Eq. (1) is best approximated, i.e., the L^2—norm of the difference of the reciprocal velocities is minimized. The velocities are determined on the one hand by the approximation from Eq. (7) and on the other hand by the velocity $v_{\text{PREM}}(x)$, calculated analytically via Eq. (3) using the polynomials given in the PREM. This is a bit tedious but straightforward, ending up in a function for $v^2_{\text{PREM}}(x)$, which is piecewise defined in powers of x from -1 to 5 and which is continuously differentiable. Minimizing the function $f(x_1, \hat{g})$, which is defined as

$$f(x_1, \hat{g}) = \int_0^1 dx \left(\frac{1}{v(x, x_1, \hat{g})} - \frac{1}{v_{\text{PREM}}(x)} \right)^2, \tag{8}$$

corresponds to a weighted fit of the velocity profile, where the weights take into account that smaller velocities make a greater contribution to the accumulated time.

The function $f(x_1, \hat{g})$ can be minimized numerically using a standard optimization procedure (e.g., Nelder–Mead) and gives $x_1 = 0.49$ and $\hat{g} = 1.055$ ($\mu = 0.107$). The minimum of $f(x_1, \hat{g})$ is not very sensitive to small changes of these parameters and the mean error of this approximation is just $\sigma \approx 3 \times 10^{-3}$.

The quality of the approximation can be seen in Fig. 2, where the approximation given in Eq. (7) coincides very well with the more complex v_{PREM}. A detail enlargement in Fig. 2 and in the following figures makes this even clearer. Close to the transition from the outer to the inner core ($x = 1221.5/6371 = 0.19$), the assumption of constant gravity

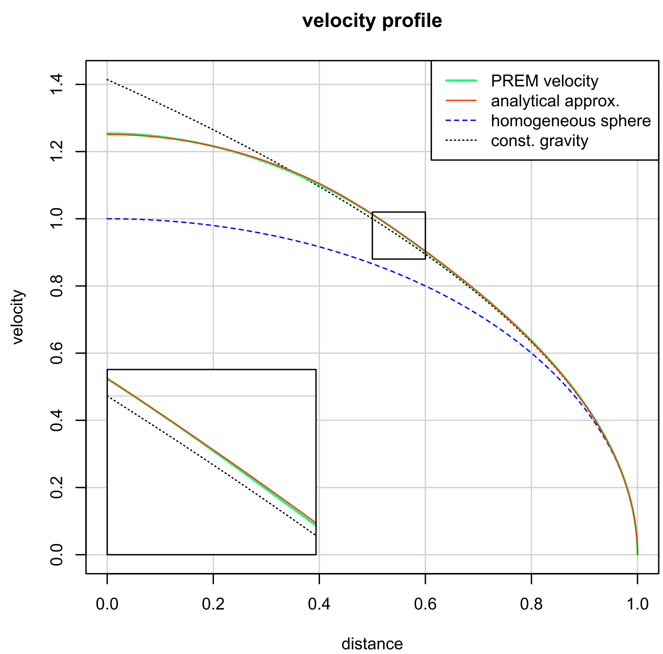

Fig. 2. Velocity profile of the Earth deduced from the PREM and the analytical approximation, compared to a homogeneous sphere and to the case of constant gravity in normalized coordinates. The quality of the approximation is illustrated by the detail enlargement.

may serve as a suitable approximation as well. But this approximation does not show the flat maximum of the velocity at the center of the Earth, which is due to zero gravity at the center. Starting with zero velocity at the surface, the maximum velocity at the center $v(0) = (1 + \hat{g} - x_1)^{1/2} = 1.25$ is between the maximum velocity of an Earth with constant density ($v(0, x_1 = 0, \mu = -1) = 1$) and constant gravity ($v(0, x_1 = 0, \mu = 0) = 1.41$), where constant gravity at the Earth's center is impossible.

III. SHORTEST PATH

The shortest path between two points on the surface of the Earth is a straight line through the Earth. Without restriction of generality the orientation of the path is described by the minimal distance d to the Earth's center or the central angle $2\theta_0$, which equals the distance between two points at the surface in normalized coordinates and is related to d by $d = \cos\theta_0$ (see Fig. 3).

The solution for the time dependence is expressed in terms of trigonometric functions and Legendre elliptical integrals $F(\varphi, k)$, $E(\varphi, k)$ and $\Pi(\varphi, n, k)$, of the first, second, and third kinds. Here, we follow the notation of Gradshteyn and Ryzhik,[9] where k is called the modulus of the integrals and n is the parameter of the integral of the third kind. In the case of $\varphi = \pi/2$, the integrals $K(k)$, $E(k)$ and $\Pi(n, k)$ are called complete elliptic integrals of the first, second, and third kind.

Integrating Eq. (1) with

$$t = \int \frac{dy}{v\left(\sqrt{d^2 + y^2}\right)}, \tag{9}$$

where d is the minimal distance of the path to the Earth's center, y is the displacement perpendicular to the axis of symmetry in the range between $-(1 - d^2)^{1/2}$ and $(1 - d^2)^{1/2}$, and v is the approximation from Eq. (7), we get for the traversal time T on a straight path in normalized units

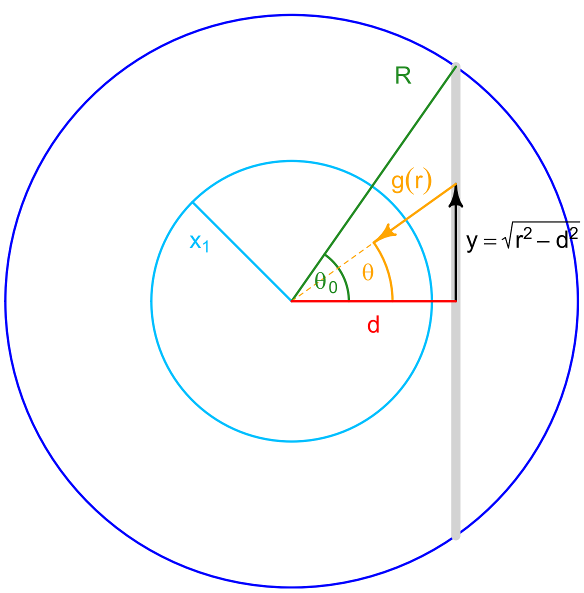

Fig. 3. Illustration of the coordinate system used in the analytical calculations.

$d \le x_1$

$$\begin{aligned} T &= \frac{4}{\sqrt{\left(2 + \mu(1-d)\right)(1+d)}} \\ &\quad \times \left(\left(1 + \frac{2}{\mu}\right)K(k) - \frac{2}{\mu}\Pi(n,k)\right), \\ &\text{where } n = \mu\frac{1-d}{2+\mu(1-d)}, \\ k &= \sqrt{\frac{1-d}{1+d}\frac{2+\mu(1+d)}{2+\mu(1-d)}}, \end{aligned} \tag{10a}$$

$d \le x_1$

$$\begin{aligned} T &= \frac{4}{\sqrt{\left(2 + \mu(1-d)\right)(1+d)}} \\ &\quad \times \left(\left(1 + \frac{2}{\mu}\right)F(\varphi,k) - \frac{2}{\mu}\Pi(\varphi,n,k)\right) \\ &\quad + \frac{2}{\omega}\sin^{-1}\left(\frac{\omega\sqrt{x_1^2 - d^2}}{v_d}\right), \\ &\text{where } \varphi = \sin^{-1}\sqrt{\frac{1-x_1}{1-d}\frac{2+\mu(1-d)}{2+\mu(1-x_1)}}, \\ \omega &= \sqrt{\frac{\hat{g}}{x_1}}, \quad v_d = \sqrt{1 + \hat{g} - x_1 - \omega^2 d^2}\,. \end{aligned} \tag{10b}$$

In the limit $\mu \to 0$ in Eq. (10a), we get the traversal time T_c for constant gravity

$$T_c = 2\sqrt{\frac{2}{1+d}}\left((1+d)E(k) - dK(k)\right). \tag{11}$$

One may notice that Eq. (11) differs from that given in Eq. (A10) in Ref. 5 by the sign of $dK(k)$. The correct sign can be checked by evaluating Eq. (11) with $d = 1$ and $k = 0$, which gives the correct value π in Eq. (11) but 3π in Eq. (A10) in Ref. 5.

The influence of the slightly increasing gravitation is made clear by a series expansion of Eq. (10a) in $\delta = 1 - d$

$$\begin{aligned} T = \pi\Bigg(1 &- \frac{1+\mu}{8}\delta + \frac{(1+\mu)(1+9\mu)}{256}\delta^2 \\ &+ \frac{(1+\mu)\left(15 - 2\mu - 25\mu^2\right)}{2048}\delta^3 + \cdots\Bigg). \end{aligned} \tag{12}$$

In the case $\mu = 0$, Eq. (12) is the series expansion of Eq. (11), and for $\mu = -1$ we identify the case of a homogeneous sphere with a constant traversal time $T_{\rho = const} = \pi$ independent of d. Figure 4 shows the difference between constant and slightly increasing gravity, which is maximized when the distance d of the path is close to the transition zone of the lower shell and the outer core. When passing the outer core, the motion changes to a harmonic oscillation with frequency ω, reaching the maximum velocity of v_d at the minimal distance d.

In the case of $d = 0$, the equation of motion simplifies for $y \ge x_1$

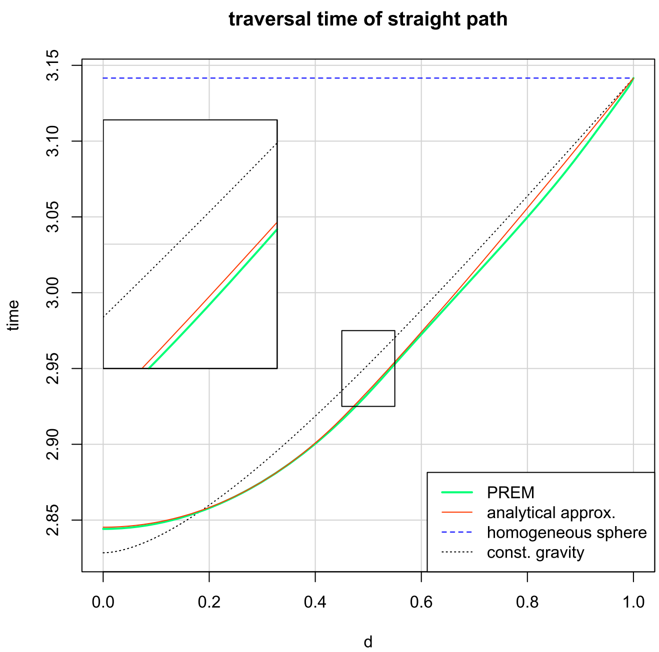

Fig. 4. Comparison of the PREM model, the described approximation and the case of constant gravity and linear decreasing gravity of a homogeneous sphere. Distance d from the center is measured in units of R and time in units of $(R/g)^{1/2}$.

$$y = 1 - \frac{2}{\mu}\sinh^2\left(\frac{\sqrt{\mu}}{2}t_1\right) = 1 - \frac{t_1^2}{2} + \mu\frac{t_1^4}{24} + \cdots, \tag{13}$$

for $x \le x_1$

$$y = x_1\cos(\omega t_2) - v_{x_1}\sin(\omega t_2), \tag{14}$$

where we count t_1 and t_2 from zero. The leading term in μ in Eq. (13) gives the correction to the case of constant gravity, which is recognized for $\mu = 0$. For $\mu = -1$, it is just the expansion of $\cos(t_1)$ as expected. Assuming $\omega t_2 \ll 1$ the harmonic oscillation is approximated by

$$y = x_1 - v_{x_1}t_2 - \frac{1}{2}\hat{g}t_2^2 + O\left((\omega t_2)^3\right). \tag{15}$$

The harmonic oscillation initially behaves like a downward motion with initial velocity $v_{x_1} = ((1+\hat{g})(1-x_1))^{1/2}$ and constantly accelerated with $\hat{g}$.

The traversal time T_0 for $d = 0$ is given by

$$T_0 = 2\left(\frac{2}{\sqrt{\mu}}\sinh^{-1}\left(\sqrt{\frac{\mu}{2}(1-x_1)}\right) + \frac{1}{\omega}\sin^{-1}\left(\frac{\omega x_1}{v_0}\right)\right). \tag{16}$$

Taking the values of x_1 and $\hat{g}$ for $\omega = (\hat{g}/x_1)^{1/2}$, $v_0 = (1+\hat{g}-x_1)^{1/2}$ defined in Eq. (10b) and μ defined in Eq. (6), we get T_0 in natural units

$$T_0 = 2\,(1.0054 + 0.4173)\sqrt{\frac{R}{g}} = 2\cdot 1.4227\sqrt{\frac{R}{g}}, \tag{17}$$

while direct integration of the inverse of v_{PREM} yields a factor of 2×1.4221. The traversal time for a path through the center of the Earth is well approximated by twice the time $t_1 = 1.0054$ of free falling a distance $(1 - x_1)$ to the boundary of the outer core, accelerated by a slightly increasing gravity plus twice the time $t_2 = 0.4173$ that a harmonic oscillation with frequency ω takes to reach the center with initial position x_1 and maximum velocity v_0 at the center.

The path difference at the boundary of the outer core at time $t_1 \simeq 1$ between the models of constant gravity and slightly increasing gravity can be read from Eq. (13) and is approximately $\mu/24$ or about 29 km in natural units ($\mu R/24$), which is small but several orders of magnitude larger than the 50 m indicated in Ref. 5. This 4 second lead is lost during the harmonic oscillation with a gravity linearly decreasing from $\hat{g}$ to 0. The harmonic oscillation takes 10 s longer than a motion constantly accelerated with g. The quality of the approximation can be seen in Fig. 5, which shows the motion on straight paths, starting from different positions.

The values given by the elliptic integrals fit perfectly to those of the PREM, which are calculated by numerical integration of the analytical velocity profile. The correspondence between a movement through the real Earth and through a homogeneous analog is good as long as the movement takes place near the surface. The shading in Fig. 5 indicates this region, where the distance to the surface is less than 0.05, which causes a maximal difference of the velocity $v_{\mu>0}$ of a slightly increasing gravity of Eq. (7) and the velocity within a homogeneous sphere $v_{\rho=const} = (1 - x^2)^{1/2}$ at $x = 0.95$ of about 1%.

IV. PATH OF FASTEST DESCENT

The path of fastest descent, which is also known as the brachistochrone curve, is obtained via the calculus of variations.

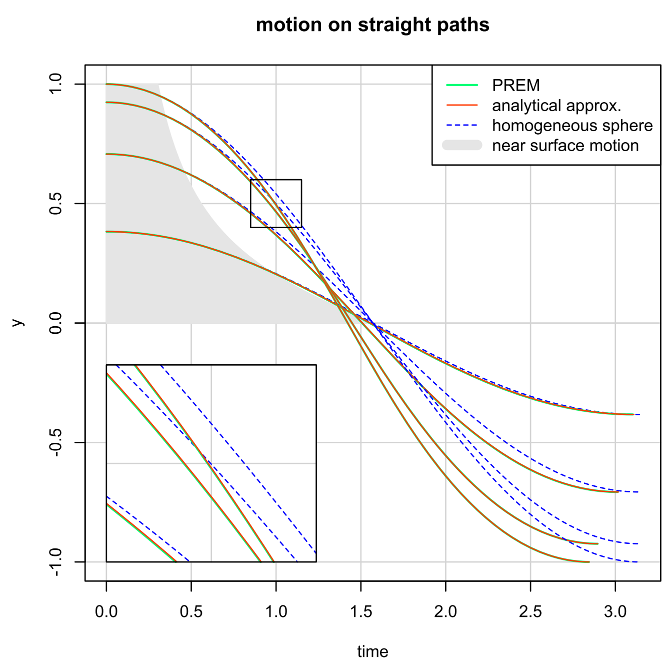

Fig. 5. The integrated equation of motion on straight paths for the PREM and for the analytical approximation, which differ from those of a homogeneous sphere especially for a motion, that is not close to the surface. Different starting positions are chosen with $y_0 = \sin\theta_0$ and $\theta_0 \in \{\pi/8, \pi/4, 3\pi/8, \pi/2\}$. Distance y from the axis of symmetry is measured in units of R and time in units of $(R/g)^{1/2}$.

The rotation of the Earth gives a mean correction to the gravity of about 0.1%, which is much smaller than the correction caused by the increasing gravity in our approximation with a value of 5.5% above g at x_1. Since we neglect the rotation of the Earth, the motion proceeds in a plane. We use polar coordinates for the path element ds in Eq. (1)

$$t = \int \frac{\sqrt{dr^2 + r^2 d\theta^2}}{v(r)} = \int d\theta \frac{\sqrt{r'^2 + r^2}}{v(r)}. \tag{18}$$

The integral does not depend explicitly on θ, so that the Euler-Lagrange equation of the functional

$$\mathcal{L} = \frac{\sqrt{(dr/d\theta)^2 + r^2}}{v(r)} \tag{19}$$

reduces to the Beltrami identity, which gives

$$\frac{r^2}{v(r)\sqrt{(dr/d\theta)^2 + r^2}} = \tau = \frac{d}{v(d)}. \tag{20}$$

Here, τ is a constant of the path and $v(d)$ is the maximum velocity at the axis of symmetry, where the distance to the center is minimal and equals d, and $dr/d\theta$ equals zero. From Eqs. (18) and (20), we get

$$\theta = \int dr \frac{\tau v(r)}{r\sqrt{r^2 - \tau^2 v^2(r)}} \tag{21}$$

and

$$t = \int dr \frac{r}{v(r)\sqrt{r^2 - \tau^2 v^2(r)}}. \tag{22}$$

If we calculate the definite integral of Eq. (21) in the limits from d to 1 in normalized units and insert the dimensionless velocity $v(x)$ from Eq. (7), we get for
$d \geq x_1$:

$$\theta_0 = 2(1-k)(\Pi(k,k) - \Pi(q,k)), \tag{23a}$$

$d \leq x_1$:

$$\theta_0 = 2(1-k)(\Pi(\varphi,k,k) - \Pi(\varphi,q,k)) + \tan^{-1}\left(\frac{a}{d}\sqrt{\frac{x_1^2 - d^2}{a^2 - x_1^2}}\right) - \frac{d}{a}\tan^{-1}\left(\sqrt{\frac{x_1^2 - d^2}{a^2 - x_1^2}}\right), \tag{23b}$$

where

$$k = \frac{(1-\gamma)(2+\mu)}{2+\mu(1-\gamma)}, \quad q = \frac{\mu}{2+\mu}k,$$

$$\varphi = \sin^{-1}\sqrt{\frac{(2+\mu(1-\gamma))(1-x_1)}{(2+\mu(1-x_1))(1-\gamma)}},$$

$$a = \sqrt{\frac{x_1(1+\hat{g}-x_1)}{\hat{g}}} = \frac{v_0}{\omega}.$$

Here, γ is the positive root in the interval [0, 1] of the quadratic equation $x^2 v^2(d) - d^2 v^2_{x \geq x_1}(x) = 0$, which gives $\gamma = d$ in the case of $d \geq x_1$ and is slightly greater than d in the case of $d < x_1$.

Inverting the series expansion of θ_0 in $1 - d$ for $d \geq x_1$ in Eq. (23a) gives

$$d = 1 - 2\frac{\theta_0}{\pi} - (1+\mu)\left(\frac{\theta_0}{\pi}\right)^2 + \frac{(1+\mu)(2+\mu)}{2}\left(\frac{\theta_0}{\pi}\right)^3 + \frac{(1+\mu)(2+\mu)(6+\mu)}{8}\left(\frac{\theta_0}{\pi}\right)^4 + \cdots, \tag{24}$$

which shows that the minimal distance d of the path to the center for a given θ_0 is reduced by a small amount of second order in θ_0/π, compared to the case of the homogeneous sphere ($\mu = -1$) with $d = 1 - 2\theta_0/\pi$. The deviation of the path has a maximum of about 0.04 near $d \simeq x_1$ and $\theta_0 \simeq \pi/4$. Figure 6 shows the evaluation of Eq. (23), which coincides with the PREM solution. The correction of the path due to the slightly increasing gravity is an order of magnitude smaller than the correction due to constant gravity compared to linear decreasing gravity of a homogeneous sphere. The solution for θ_0 in the region $d \geq x_1$ may also be approximated by the constant gravity assumption; setting $\mu = 0$ in Eq. (23a) gives

$$\theta_{0_{\mu=0}} = 2d(\Pi(1-d, 1-d) - K(1-d)). \tag{25}$$

The inverse trigonometric functions in the solution for θ_0 in the region $d < x_1$ result from the approximation of linear decreasing gravity. Here, a determines the radius of a homogeneous sphere with gravitation $\hat{g}/x_1$ so that the magnitude of the velocity profile of a homogeneous sphere corresponds to the value of the velocity profile of the Earth at radius x_1, which is $v(x_1) = ((1+\hat{g})(1-x_1))^{1/2}$. As described in Ref. 3, the path then is a hypocycloid generated by a circle of radius $(a - d)/2$ rolling inside a circle of radius a. The path

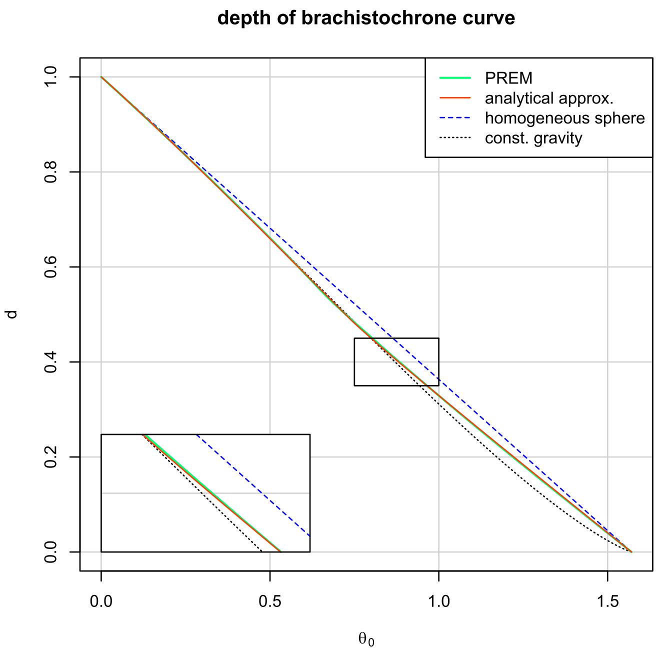

Fig. 6. The maximum depth $1 - d$ of the fastest path starting at initial θ_0 is increased compared to the path through a homogeneous sphere.

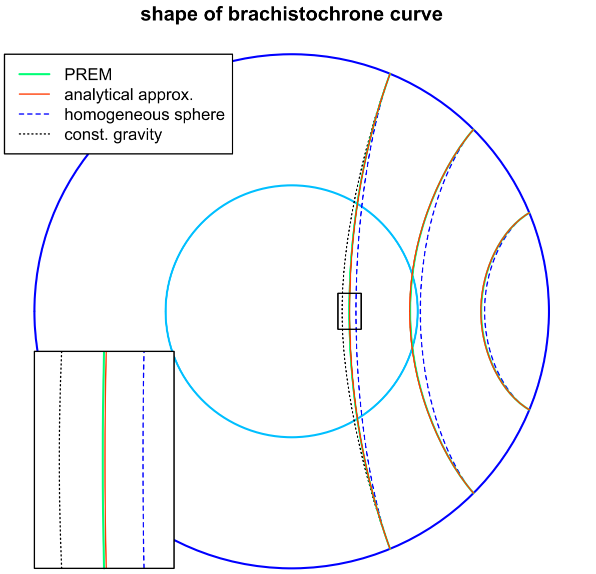

Fig. 7. Comparison of the shapes of the fastest paths for different models. Different starting positions are chosen with $\theta_0 \in \{\pi/8, \pi/4, 3\pi/8\}$. The inner circle indicates the zone of rapidly decreasing gravity.

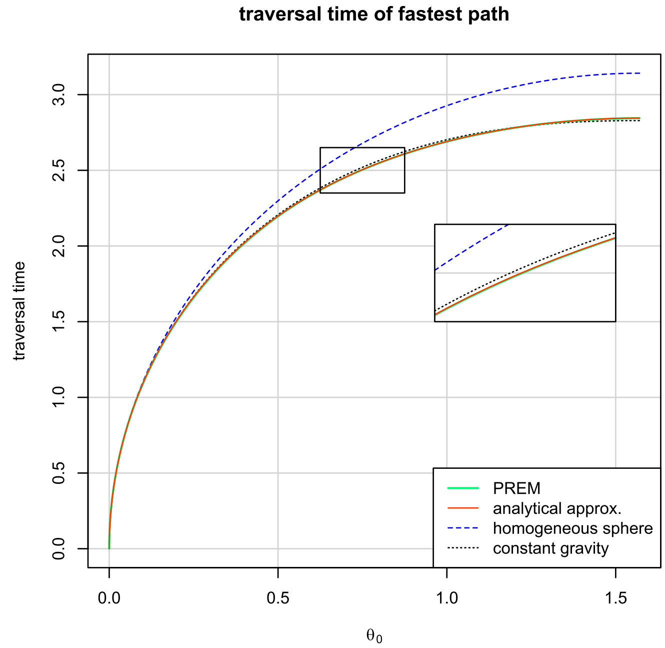

Fig. 8. Dependence of the traversal time of the brachistochrone curve in units of $(R/g)^{1/2}$. θ_0 is proportional to the distance $l = 2R\theta_0$ at the Earth's surface.

is shorter than a corresponding path assuming constant gravity. Figure 7 shows the comparison of paths with different starting points.

In the same way that we calculated θ_0 we calculate the traversal time of the fastest path through the earth via Eq. (22) and get the following result:

$d \geq x_1$:

$$T = 2\sqrt{\frac{4k}{2+\mu}}\left(\left(1+\frac{2}{\mu}\right)K(k) - \frac{2}{\mu}\Pi(q,k)\right), \tag{26a}$$

$d \leq x_1$:

$$T = 2\sqrt{\frac{4k}{2+\mu}}\left(\left(1+\frac{2}{\mu}\right)F(\varphi,k) - \frac{2}{\mu}\Pi(\varphi,q,k)\right) + 2\sqrt{\frac{a^2-d^2}{1+\hat{g}-x_1}}\tan^{-1}\sqrt{\frac{x_1^2-d^2}{a^2-x_1^2}}. \tag{26b}$$

Here, φ, q, k, and a have the same meaning as in Eq. (23). A series expansion in $\delta = 1 - d$ of the traversal time T in the region $d \geq x_1$ gives

$$T = \pi\sqrt{2\delta}\left(1 - \frac{2+\mu}{4}\delta + \frac{(2+\mu)(4+5\mu)}{32}\delta^2 + \cdots\right). \tag{27}$$

Substituting $\mu = -1$ into Eq. (27) yields the series expansion of $T_{\rho=const.} = \pi(1-d^2)^{1/2}$ at $d = 1$, which is the traversal time of the fastest path through a homogeneous sphere with minimum distance d from the center.[3] In the case $\mu = 0$ Eq. (27) represents the series expansion of

$$T_{\mu=0} = 2\sqrt{\frac{2}{1-d}}(E(1-d) - dK(1-d)), \tag{28}$$

which is the limit $\mu \to 0$ of Eq. (26a) and represents the traversal time under the assumption of constant gravity. One may notice that Eq. (28) looks much simpler than the corresponding Eq. (A6) given in Ref. 5 (obtained via CAS Maple), without extending the solution into the complex plane.

Figure 8 shows the comparison of the different solutions. Since the paths are different for a given θ_0, the traversal time is plotted against θ_0 instead of d. Substituting the series expansion of d in Eq. (24) into Eq. (27), we obtain for small θ_0/π

$$T = 2\pi\sqrt{\frac{\theta_0}{\pi}}\left(1 - \frac{3+\mu}{4}\frac{\theta_0}{\pi} - \frac{1+6\mu-3\mu^2}{32}\left(\frac{\theta_0}{\pi}\right)^2 + \frac{13+33\mu+11\mu^2-\mu^3}{128}\left(\frac{\theta_0}{\pi}\right)^3 + \cdots\right). \tag{29}$$

Substituting $\mu = -1$ in Eq. (29), we obtain the series expansion of the traversal time of the brachistochrone curve for the case of constant density which is given in Ref. 3

$$T_{\rho=\text{const.}} = 2\pi\sqrt{\frac{\theta_0}{\pi}\left(1-\frac{\theta_0}{\pi}\right)}. \tag{30}$$

The traversal time is a smooth function of θ_0 in all models, in contrast to the calculations in Ref. 5, which show small fluctuations for the PREM that are probably caused by numerical inaccuracy. From Eq. (29), it can be seen that for small $\theta_0 < 0.1$ the traversal time of the fastest path does not vary between models of constant density, constant gravity and slightly increasing gravity within an accuracy of 1% ($\mu\theta_0/4\pi$ with μ varying from -1 to 0.11). On a brachistochrone curve with $\theta_0 = \pi/4$, the slightly increasing gravity results in a travel time that is only about 1% ($\mu/16$) less compared to the model of constant gravity. For a path with $d \leq x_1$ the velocity for constant gravity and linear decreasing gravity up to a radius of 0.3 is nearly the same as shown in

Fig. 2. For a path closer to the center, the higher velocity in a constant gravity model is partly compensated by a longer path, which leads to a maximum difference of 0.6% in traversal times at $d = 0$ as described in Sec. III.

Moreover, the motion near the surface does not differ in the models. At each starting point, the brachistochrone curve points directly to the center of the earth, which results in the maximum acceleration. So the time reaching a depth of $1 - r = 0.05$ is nearly equal for all path with $d < 0.95$. This region is shown in Fig. 9. Since the motion takes place in a plane, only the coordinate that is perpendicular to the axis of symmetry is displayed in the figure.

V. COMPUTATIONAL DETAILS

Numerical integration, optimization and figures are performed in R.[10] Evaluations of series expansions are supported by Maxima.[11] All analytical solutions containing elliptical integrals are taken from Gradshteyn and Ryzhik[9] and have been verified by numerical integrations. Numerical evaluations of the elliptic integrals are performed by algorithms for symmetric forms of elliptic integrals of first, second, and third kind as proposed by Carlson.[12]

VI. CONCLUSION

We have described solutions of paths through an inhomogeneous earth by a combination of inverse trigonometric functions and elliptic integrals. The elliptical integrals that provide the solution for slightly increasing gravity ($\mu > 0$) include the solution for constant gravity ($\mu = 0$) and constant density ($\mu = -1$). The good approximation of travel time by the assumption of constant gravity is confirmed.

The reason is not a radius squared mass profile. A log fit gives an exponent of 2.96 up to the limit of the outer core, approximately for the first half, and an exponent of 1.96 for the second half, as one would expect from the gravity profile shown in Fig. 1. Moreover, on the way to the center of the Earth, the time spent in the region of rapidly decreasing gravity is smaller (ratio 30:70), but of the same order of magnitude as in the upper half.

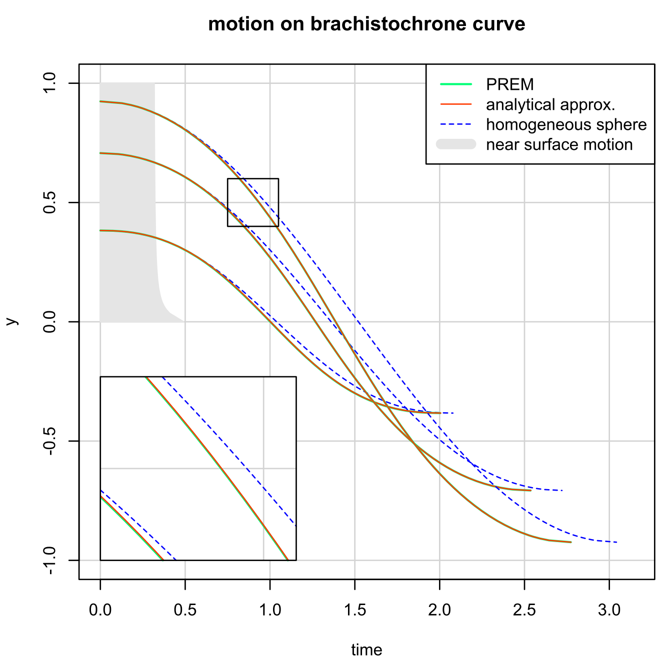

Fig. 9. Comparison of motion on a brachistochrone curve for the PREM, the analytical approximation and a sphere with constant density. The displacement $y = r(t)\sin\theta(t)$ perpendicular to the axis of symmetry with different starting positions $y_0 = \sin\theta_0$ and $\theta_0 \in \{\pi/8, \pi/4, 3\pi/8\}$ is shown; y is measured in units of R and time in units of $(R/g)^{1/2}$.

The change in gravity does not result in a similar change of speed, because velocity is the result of the integrated gravity, which can be seen directly from Fig. 2. The change in gravity occurs at $x \approx 0.5$, while the change in velocity becomes apparent at $x \approx 0.3$. This holds for the transition from constant to linear decreasing gravity at the surface as well as at the beginning of the outer core. Further integration of velocity reduces differences in the time dependence of the different models once again. This is reflected by the fact that traversal times do not depend on the shape of gravity in the leading order. And the motion at the transition from constant to linear decreasing gravity does not differ much for small variations $\Delta r < 0.1$ of the distance to the center of the Earth. This applies to the different models with constant gravity and constant density at the Earth's surface as well as to the transition zone at the outer core from nearly constant gravity to linear decreasing gravity. The velocities at the center of the Earth, however, differ significantly. We get 1 for constant density, 1.25 for PREM and 1.41 for constant gravity or in natural units 7.9 km/s, 9.9 km/s, and 11.2 km/s, respectively.

The parameters x_1 and $\hat{g}$ of the given solutions can easily be adapted to other terrestrial profiles, even if this may only be of academic interest. The traversal times should always be dominated by the parameters radius R and surface gravity g of the planet. The traversal time for the path through the center of terrestrial planets, which are primarily composed of a core of metal and a mantle of silicate rock, should be little larger than for the Earth, in units of $(R/g)^{1/2}$ specific to the planet, provided that the metal core has a significantly smaller (moon) or larger (Mercury) extent than that of the Earth. The density of such planets tends more toward the case of constant density and therefore to the upper limit of the traversal time $T_{\max} = \pi(R/g)^{1/2}$. Assuming an uncompressed iron core (8 g/cm^3) with an extension of 20% of the radius for the moon and 80% for Mercury and a mantle of silicate rock (3 g/cm^3), we get traversal times in dimensionless units of 3.10 and 2.88, respectively. Traversal times of about 2.85 are typical for terrestrial planets with an iron core of roughly 50%, regardless of their exact internal structure.

Depending on the mass concentration, this simple model allows for traversal times which are even smaller than a traversal time resulting from the assumption of constant gravity as shown in Fig. 10.

It is obvious that traversal times become shorter the more mass of the planet is located near the center. If almost the entire mass is located near the center, the mass profile rises from zero to almost its total mass in a short distance and remains almost constant up to the surface. This is also considered as the limiting case of the model of polytropes in Ref. 4. Therefore, the gravity varies with $1/r^2$ over almost the entire range, and the theoretical lower bound of a traversal time starting with zero velocity at the surface and passing the center is given by

$$T_{\min} = 2\sqrt{\frac{R}{g}}\int_0^1 dx\sqrt{\frac{x}{2(1-x)}} = \frac{\pi}{\sqrt{2}}\sqrt{\frac{R}{g}}. \tag{31}$$

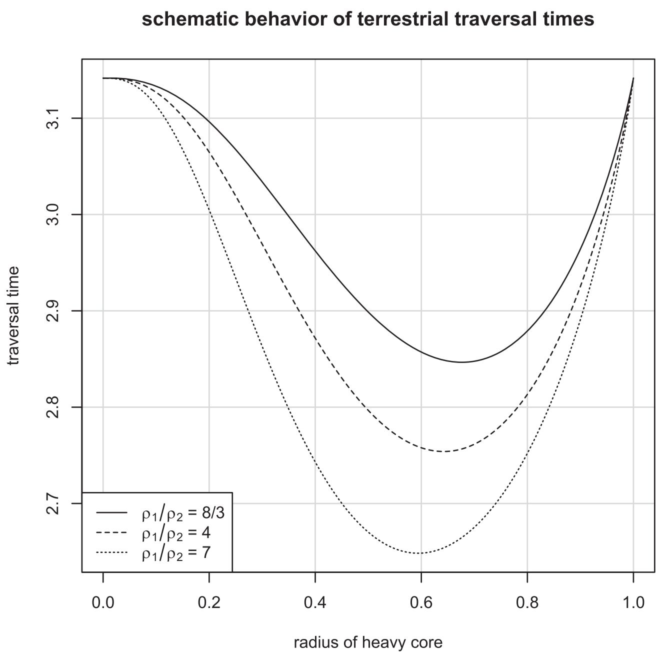

Fig. 10. Traversal times of terrestrial planets for different density ratios ρ_1 (heavy core) to ρ_2 (light mantle) depending on the size of the core. Traversal time is measured in units of $(R/g)^{1/2}$ and the size of the core in units of R.

It is known that $T_{\min}$ is twice the proper time of free falling into the singularity of a black hole from a distance R where the gravity is g. But this is a journey without return after passing the event horizon at $2gR^2/c^2$ (c is the velocity of light).[13] Therefore, the maximum variation of traversal times is about 30% in units of $(R/g)^{1/2}$, unless there is an anomaly in the density profile, i.e., an increase of density from the center to the surface.

[1]M. Selmke, "A note on the history of gravity tunnels," Am. J. Phys. **86(2)**, 153 (2018).
[2]H. Goldstein, C. P. Poole, and J. L. Safko, *Classical Mechanics*, 3rd ed. (Addison-Wesley, Boston, 2001), ex. 2.6.
[3]G. Venezian, "Terrestrial brachistochrone," Am. J. Phys. **34**(8), 701 (1966).
[4]W. D. Pesnell, "Flying through polytropes," Am. J. Phys. **84**(3), 192–201 (2016).
[5]A. R. Klotz, "The gravity tunnel in a non-uniform Earth," Am. J. Phys. **83**(3), 231–237 (2015).
[6]A. M. Dziewonski and D. L. Anderson, "Preliminary reference Earth model," Phys. Earth Planetary Interiors **25**(4), 297–356 (1981).
[7]T. G. Concannon and G. Giardo, "Gravity tunnel drag," <https://arxiv.org/pdf/1606.01852.pdf> (2016).
[8]A. J. Simoson, "Falling down a Hole through the Earth," Math. Mag. **77(3)**, 171–189 (2004).
[9]I. S. Gradshteyn and L. M. Ryzhik, *Table of Integrals, Series, and Products*, edited by D. Zwillinger and V. Moll, 8th ed. (Academic Press, San Diego, 2014).
[10]R Core Team, "R: A language and environment for statistical computing," R Foundation for Statistical Computing, Vienna, Austria (2017). <https://www.R-project.org/>
[11]Maxima, a Computer Algebra System. Version 5.41.0 (2017). <http://maxima.sourceforge.net/>.
[12]B. C. Carlson, "Numerical computation of real or complex elliptic integrals," Numer. Algorithms **10**, 13–26 (1995).
[13]C. W. Misner, K. S. Thorne, and J. A. Wheeler, *Gravitation* (W. H. Freeman, San Francisco, 1973).

Watt's External Condenser

We think that James Watt invented the steam engine, but he actually started by devising the external condenser. In earlier steam engine designs, such as the Newcomen engine, steam was used to lift the piston against its own weight. Cold water sprayed into the cylinder condensed the steam into water, and gravity pushed down the piston to its starting point. The external condenser was an extension of the system, and cold water sprayed onto the outside caused the steam to condense. The advantage here is that the cylinder did not have to be heated up each time. This model is at Baldwin Wallace University in Berea, Ohio. The bulb has a small amount of water in it that is first heated, producing steam and pushing out the piston; putting the bulb under a steam of cold water caused the piston to move inward. (Picture and text by Thomas B. Greenslade, Jr., Kenyon College)